metals

MDPI

Article

Joining Stainless-Steel AISI 304 and High-Strength Aluminum Alloy AA 6082 by Brazing Using Al-Ge-Si Foils

Alexander Ivannikov, Anton Abramov *, Nikita Popov, Milena Penyaz, Alexey Suchkov, Natalia Pukhareva and Oleg Sevryukov

Department of Materials Science, National Research Nuclear University (MEPhI), 115409 Moscow, Russia
* Correspondence: aav025@campus.mephi.ru; Tel.: +7-9651043982

Abstract: An Al-40.0Ge-3.4Si wt.% alloy foil with a thickness of 50 ± 5 μm, obtained via an ultrafast solidification method, is described in this work. A complete wetting of the aluminum alloy substrate with a wetting angle of 0° is observed, and the formation of a drop with a wetting angle of 30 ± 5° is observed on the steel substrate. Similar and dissimilar brazed joints of aluminum alloy AA 6082 and stainless-steel AISI 304 are obtained. The microstructure of the AA 6082/AA 6082 brazed seam is homogeneous and contains particles of an Al_7Fe_2Si system intermetallic compound and particles of an Al-Ge eutectic composition. The brazed seam of the AISI 304/AISI 304 joint is formed due to the formation of the Al_8Fe_2(Si, Cr) intermetallic compound reaction layer on the steel surface. The proposed scheme for the AISI 304/AA 6082 brazed joint formation is given. The brazed seam represents the Al_8Fe_2(Si, Cr) reaction layer on the steel surface, the thickness of which depends on the holding time during brazing, and the aluminum matrix of which has particles of a composition close to an Al-Ge eutectic. The obtained results could be used for the optimization of time–temperature brazing modes in order to improve the mechanical characteristics of AISI 304/AA 6082 dissimilar joints.

Keywords: stainless-steel AISI 304; high-strength aluminum alloy AA 6082; rapidly quenched Al-Ge-Si filler metals; wetting experiments; brazed joint; dissimilar joint; microstructure formation; mechanical properties; failure mechanisms

Citation: Ivannikov, A.; Abramov, A.; Popov, N.; Penyaz, M.; Suchkov, A.; Pukhareva, N.; Sevryukov, O. Joining Stainless-Steel AISI 304 and High-Strength Aluminum Alloy AA 6082 by Brazing Using Al-Ge-Si Foils. *Metals* **2023**, *13*, 149. https://doi.org/10.3390/met13010149

Academic Editors: Guido Di Bella, Peihao Geng and Hong Ma

Received: 29 November 2022
Revised: 24 December 2022
Accepted: 4 January 2023
Published: 11 January 2023

1. Introduction

Dissimilar joint creation is usually defined by the necessity of using the individual advantages of different materials [1]. Due to the good mechanical characteristics of stainless steel and the low relative weight of aluminum alloys, these products are of particular interest to the transport industry [2,3]. It has been hypothesized that combining aluminum alloys and steel could make it possible to produce structures combining the useful characteristics of both materials [4,5]. Such a structure could have broad application potential in various fields of industry, and could increase fuel economy [6]. However, significant differences in the thermophysical properties of these materials, such as the melting point, coefficient of thermal expansion, and thermal conductivity, are significantly complicating their connection, and result in stresses in the junction zone [7,8]. The formation of brittle Fe-Al system intermetallic compounds could seriously reduce the strength of joints [2,9,10].

There are various methods for obtaining permanent aluminum alloys and steel joints, including friction welding [11–13], arc brazing–welding [7,14], and laser welding [8,15,16]. However, these methods are often limited by the geometry of the connecting parts and lead to local melting of the base material [17]. Compared with welding, brazing methods allow us to obtain compounds of a complex shape. In addition, it is possible to reduce the connection temperature due to the fact that the liquidus temperature of the filler alloy is always lower than the solidus temperature of the base material. Selecting an optimal

time for thermal exposure and decreasing the temperature of the connection allows the obtainment of joints with good mechanical properties [17].

The liquidus temperatures of classical Al-Si system filler alloys are higher than the solidus temperatures of high-strength aluminum alloys of the Al-Mg-Si system (550–600 °C). This limits their use without additional alloying. Alloys of the Al-Si-Zn system with a melting point less than 550 °C demonstrate good properties during heat treatment. However, the zinc content causes erosive effects in the aluminum material [18]. The melting point of alloys of the Al-Si system can also be reduced by alloying Cu [19]. However, the presence of Cu leads to the formation of brittle Al2Cu intermetallic phases during brazing [20,21].

Filler alloys of the Al-Ge-Si system with a melting point lower than 500 °C can decrease the brazing temperature of aluminum alloys [22]. The use of Ge as an alloying element in the classical Al-Si system has been considered due to the low melting point of the Al-Ge system eutectic (420 °C), as well as its good wettability in terms of the aluminum substrate. Alloys with low and high Ge content have been developed [23,24]. Kawamoto [24] obtained an AA 6061 brazed joint with a strength corresponding to the base material strength.

The production of filler alloys via the ultrafast solidification (spinning) of the flat melt jet is an example of the successful application of rapidly quenching technology [25–30]. Rapid quenching of the melt allows filler alloys of the Al-Ge-Si system to be obtained with any germanium content in the foil form. Obtaining filler alloys in the rapidly quenched foil form usually leads to the conduct of brazing with minimal erosion and changes in the base material properties. Ultrafast cooling of the melt forms an homogeneous and uniform distribution of alloying components in the solidified alloy. The efficiency of the component distribution in the brazed seam increases as a result of the high chemical uniformity of the obtained rapidly quenched foils. A decrease in brazing defects and an increase in the strength of the joints brazed with rapidly quenched alloys have been observed [31,32].

The formation of Al-Fe and Al-Fe-Si systems' intermetallic reaction layers has been observed on the heterogeneous junction surface of the aluminum alloys and the stainless-steel brazed joint [2,7,33,34]. These intermetallic compounds are considered to be the main reason for the mechanical destruction of such compounds [35]. In several papers, it has been determined that the thickness of reaction layers depends on the temperature and duration of thermal exposure [36,37]. The thickness of the intermetallic layer has a significant effect on the strength of the aluminum alloys and stainless-steel joints during tensile tests. If the thickness of the intermetallic layer is >10 μm, the mechanical characteristics of the compounds sharply decrease [2,38]. In addition to reducing the temperature and duration of brazing, alloying with elements such as Mg, Si, Ca, Ti, Cr, Cu, Ge, Ag, Cd, and Sb reduces the activity coefficient of aluminum in α-Fe, which leads to a decrease in Fe-Al intermetallic layer thickness [39].

Al-Ge-Si system filler alloys are promising for brazing high-strength aluminum alloys and stainless steel. The balance between the microstructure, depending on the alloying system, mechanical characteristics, and decrease in the studied filler alloy melting point, has not yet been found. Obtaining a filler alloy with a low melting point that can form a joint with good mechanical characteristics is a significant task. There are a small number of studies that systematically consider the joints of aluminum alloys and stainless steel obtained by brazing. The purpose of this work is to establish the formation of regularities of high-strength aluminum alloy AA 6082 and stainless-steel AISI 304 joints, obtained by vacuum brazing using Al-Ge-Si systems with rapidly quenched filler alloys.

2. Materials and Methods

2.1. Materials

To study the formation features of the microstructure of the brazed aluminum alloy and stainless steel, the Al-Ge-Si system alloys were obtained in the foil form with a thickness of 55 ± 5 μm via the ultrafast (10^4–10^6 K/s) solidification of a flat melt jet on a rotating copper disk. Aluminum alloy A0 (Russian standard, GOST 11069), monocrystalline germanium, and silumin were used as the initial materials to produce ingots for rapid quenching. The

initial alloy ingots were obtained via melting in an arc vacuum furnace with a tungsten non-consumable electrode with constant stirring by passing argon through the melt with a flow rate of 7 L/min. The chemical composition of filler alloy for brazing high-strength aluminum alloy AA6082 and stainless-steel AISI 304 is shown in Table 1. Filler alloy foil in the initial state was used in all experiments. The temperature characteristics of filler alloys have been studied in previous works [22].

Table 1. Chemical compositions of the base materials and the filler metals.

Alloy	Alloy Composition (wt.%)										Melting Range, °C	
	Fe	Al	Cr	Ni	Mg	Mn	Si	Ge	C	Other		
AISI 304	Bal.	–	18.0	9.0	0.05	1.0	0.4	–	0.08	0.3		
AA 6082	0.5	Bal.	0.25	–	1.2	1.0	1.3	–	–	0.4	580	650
Filler alloy	<0.02	Bal.	–	–	–	–	3.4	40.0	–	–	442	474

As substrate materials for determining the wettability of materials with filler alloys, sheets of aluminum alloy AA 6082 with dimensions 40 mm × 40 mm × 3 mm and stainless-steel AISI 304 with dimensions 40 mm × 40 mm × 1.5 mm (Russian standard, GOST 23904-79) were used. The filler alloy was applied in the form of 8 layers of foil with a thickness of 55 μm and dimensions of 4 mm × 4 mm, stacked on top of each other and connected by contact-reactive welding.

Sheets of AA 6082 aluminum alloy with dimensions of 30 mm × 65 mm × 6 mm, AISI 304 stainless steel with dimensions of 25 mm × 55 mm × 1.5 mm, and the Al-40.0Ge-3.4Si wt.% alloy foil of 55 ± 5 μm thick and dimensions of 20 mm × 30 mm and 15 mm × 25 mm were used as the main materials for obtaining similar material joints. The brazing assembly scheme for similar materials of the aluminum alloy (AA 6082/AA6082) and the stainless steel (AISI 304/AISI 304) is shown in Figure 1 (Russian standard, GOST 28830-90).

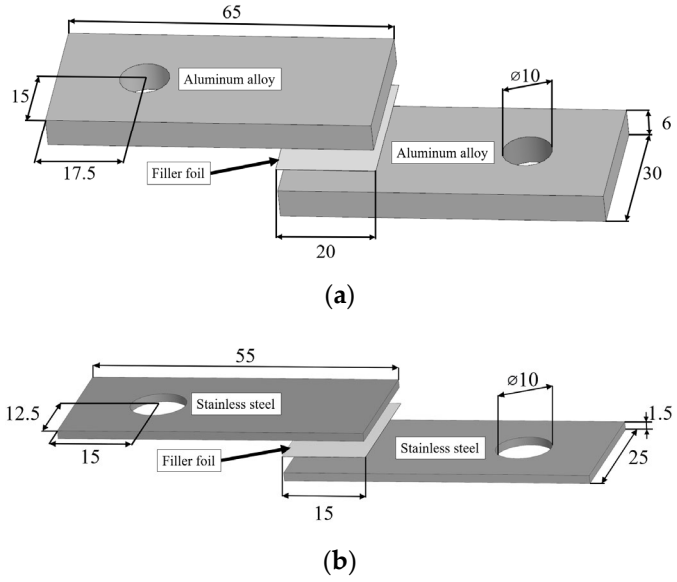

Figure 1. Brazing assembly scheme for similar materials: (**a**) AA 6082 base material; (**b**) AISI 304 base material. Values are given in mm.

Fedorov [2,35,37] obtained overlap joints of aluminum alloy AA3003 and stainless-steel AISI 304. The destruction of such joints was located in the aluminum alloy material, which does not provide information about the properties of the joint during destruction. A brazing assembly scheme for dissimilar materials, presented in Figure 2, was proposed for this reason. Sheets of AA 6082 aluminum alloy with dimensions of 15 mm × 25 mm × 3 mm

and stainless AISI 304 steel with dimensions of 25 mm × 55 mm × 1.5 mm were used to obtain dissimilar joints. One layer of filler alloy foil with a thickness of 55 ± 5 μm and dimensions of 15 mm × 25 mm was laid between the brazed materials.

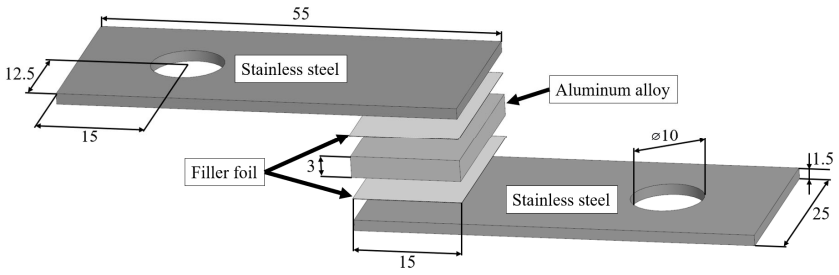

Figure 2. Brazing assembly scheme for dissimilar materials. Values are given in mm.

2.2. Methods

Before the brazing and wetting experiments, the surfaces of the main materials were cleaned with abrasive paper grit 320 and ethanol. Wetting experiments and brazing were performed in a resistance vacuum furnace SSHVE-1.2.5 (MosZETO, Moscow, Russia) under high vacuum up to 5 × 10^{-6} mmHg. The heating rate was 10 °C/min. The wetting experiments were carried out at a temperature of 540 °C above the melting point of the filler alloy for 10 min.

Brazing was carried out to form stainless-steel (AISI 304/AISI 304) and aluminum alloy (AA6082/AA6082) similar joints and dissimilar joints (AISI 304/AA6082) using the Al-40.0Ge-3.4Si wt.% filler alloy foil. Three different modes (15, 30, and 60 min) were studied at the brazing temperatures of 520 °C and 540 °C. Free cooling in high vacuum was used for all samples.

The microstructure and fractograms were analyzed via scanning electron microscopy (SEM) with a JEOL JSM-6610LV (Jeol, Tokyo, Japan) and Carl Zeiss EVO 50 XVP (Carl Zeiss, Oberkochen, Germany) at BSE observation mode. The chemical composition was analyzed via energy-dispersive X-ray spectroscopy (EDX) and a backscattered electron detector (BSD) using an INCA X-ACT (Oxford Instruments plc., Abingdon, UK) with a Carl Zeiss EVO 50 XVP (Carl Zeiss, Oberkochen, Germany) using an acceleration voltage of 10 kV.

A single-lap shear (SLS) test was conducted at room temperature. Tensile tests with a strain rate of 0.01 mm/s were carried out in a QUASAR 50 testing machine (Galdabini, Cardano al Campo, Italy), which has a maximum force of 50 kN. A total of 10 shear tests were carried out for each type of sample to clarify the results. Special steel cylindrical supports were used to ensure that the load was applied coaxially to the samples, as shown in Figures 1 and 2. Cylinders with a diameter of 10 mm and a height of 10 mm were inserted at the two ends of the samples, which allowed minimizing stress in directions perpendicular to the brazing surface.

3. Results and Discussion

3.1. Wetting Experiments

To reveal the features of the interaction mechanisms between the main materials, experiments on wetting with molten filler alloys were carried out. In a previous study [22], filler alloys of the Al-Ge-Si system in the form of ingots and foils obtained by rapid quenching were studied. These foil structures contained a eutectic structure, consisting of the (Al, Ge) solid solution and the (Si, Ge) solid solution, as well as the metastable compound Al_6Ge_5. The decomposition temperature of the metastable phase of Al_6Ge_5 was in the range of 180–240 °C, depending on the germanium and silicon content in the alloys. It was revealed that the most prospective alloy in melting point terms was Al-40.0Ge-3.4Si wt.% [22]. The wetting experiment was carried out by heating filler alloy Al-40.0Ge-3.4Si wt.% to 540 °C with exposure for 10 min. SEM images at different magnifications of the

cross-section of the AA 6082 surface wetted with the Al-40.0Ge-3.4Si wt.% filler alloy at a temperature of 540 °C are shown in Figure 3.

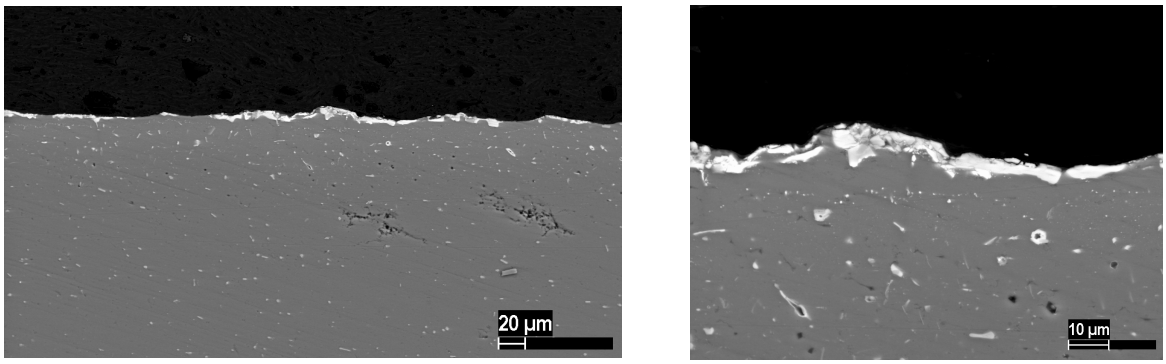

(**a**) (**b**)

Figure 3. Microstructure of AA 6082 wetted with Al-40.0Ge-3.4Si wt.% filler alloy according to 540 °C/10 min mode, obtained by SEM at various magnifications: (**a**) 500× magnification; (**b**) 1000× magnification.

The filler alloy dissolved in the base material, and the formation of bright particles close to the surface of the aluminum alloy was observed. The dissolution of the filler alloy indicates complete wetting of the aluminum substrate with a wetting angle of 0°. The results of the EDX analysis of the phases formed close to the surface of the aluminum alloy are shown in Figure 4 and in Table 2. Due to the relatively close energy on the EDX spectra, it is difficult to distinguish germanium and magnesium. This dramatically reduces the accuracy of the quantitative analysis of these elements. Due to the relatively low magnesium content in aluminum alloy AA 6082, a further study of the chemical composition was carried out without considering the Mg content.

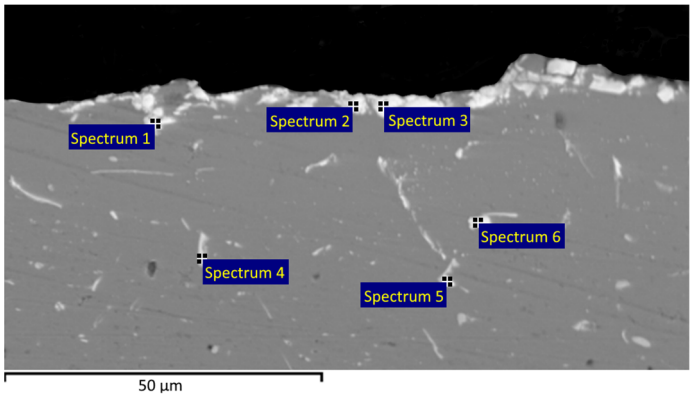

Figure 4. Microstructure of AA 6082 wetted with Al-40.0Ge-3.4Si wt.% filler alloy according to 540 °C/10 min mode with EDX measurement points.

Table 2. Results of EDX analysis of the AA 6082/Al-40.0Ge-3.4Si wt.% filler according to 540 °C/10 min mode alloy wetting experiment.

Measurement Point	Chemical Composition (at.%)				Phase Interpretation
	Al	Si	Ge	Mn	
Spectra 1–3	6.3	58.6	35.1	0.3	(Si, Ge)
Spectra 4–6	63.3	5.6	33.1	0.5	Al-Ge eutectic

Spectra 1–3 indicate that the particles on the surface were presumably a (Si, Ge) solid solution (Figure 4, spectra 1–3). The phases, which were deeper in the Al alloy, had a composition close to eutectic in accordance with the ternary Al-Ge-Si system diagram [22].

Cross-sectional SEM images of AISI 304 wetted with Al-40.0Ge-3.4Si wt.% filler alloy at 540 °C at various magnifications are presented in Figure 5. The contact angle was 30 ± 5°.

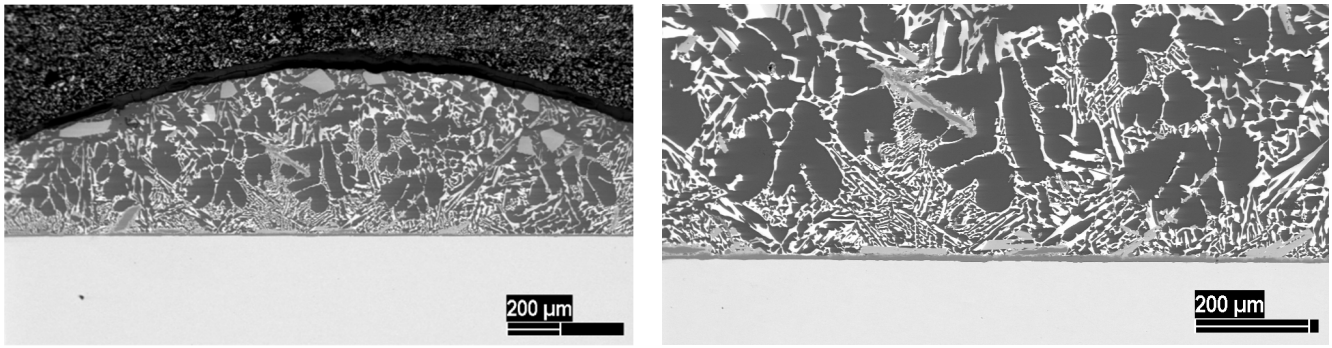

(**a**) (**b**)

Figure 5. Microstructure of AISI 304 wetted with Al-40.0Ge-3.4Si wt.% filler alloy according to 540 °C/10 min mode, obtained by SEM at various magnifications: (**a**) 50× magnification; (**b**) 100× magnification.

The results indicate the wetting of the steel substrate with a filler alloy and the formation of a chemical interaction zone. The EDX analysis was performed to study the formation of a reaction layer between a molten filler alloy and steel (Figure 6, Table 3).

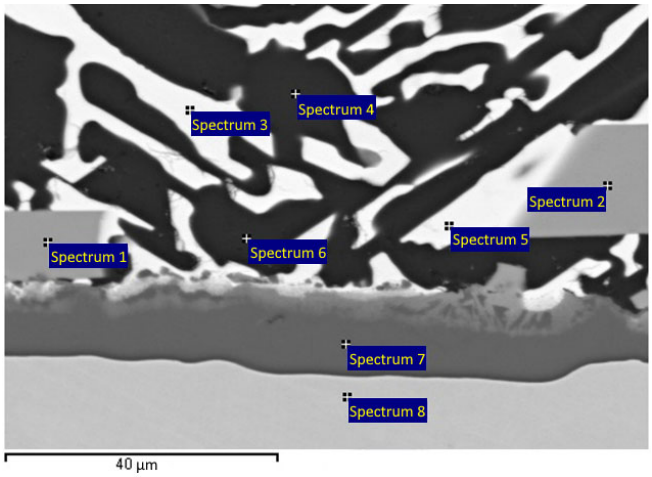

Figure 6. Microstructure of AISI 304 wetted with Al-40.0Ge-3.4Si wt.% filler alloy according to 540 °C/10 min mode with EDX measurement points.

Fedorov [2] studied the growth of the intermetallic compound layers and formation of the additional thin sublayers during heat treatment of the AA 3003/AISI 304 induction brazed joint. Similarly to the results obtained by Fedorov, the chemical composition of the phase measured, corresponding to spectrum 7 (Table 3), can be approximated by Al_8Fe_2(Si, Cr). The steel and solidified filler alloy droplet were bonded by the Al_8Fe_2(Si, Cr) intermetallic compound layer (Figure 6, spectrum 7). The formation of large ~20 µm particles corresponding to the Al-Ge eutectic in the boundary layer was also observed (Figure 6, spectra 1, 2). A structure containing two eutectics with a chemical composition similar to the Al-40.0Ge-3.4Si wt.% alloy initial ingot was formed on the droplet periphery [22]. It should be noted that germanium does not participate in the formation of the intermetallic layer, and forms phases located in the boundary areas of the contact surface of the materials.

Table 3. Results of EDX analysis of the AISI 304/Al-40.0Ge-3.4Si wt.% filler according to 540 °C/10 min mode alloy wetting experiment.

Measurement Point	Chemical Composition (at.%)							Phase Interpretation
	Al	Si	Ge	Fe	Cr	Ni	Mn	
Spectra 1, 2	66.0	1.5	28.8	3.3	0.2	–	0.2	Al-Ge eutectic
Spectra 3, 5	1.9	5.6	91.8	0.6	0.1	–	–	(Ge, Si)
Spectra 4, 6	97.6	0.6	1.7	0.1	–	–	–	(Al)
Spectrum 7	72.2	7.6	1.6	13.5	4.8	–	0.3	Al_8Fe_2(Si, Cr)
Spectrum 8	–	0.8	–	68.4	19.0	10.1	1.7	AISI 304

3.2. Similar Material Brazing

Brazing according to the 540 °C/30 min mode using Al-40.0Ge-3.4Si wt.% filler alloy foil was carried out to establish the mechanisms of the aluminum alloy (AA 6082/AA6082) joint formation (Figure 7).

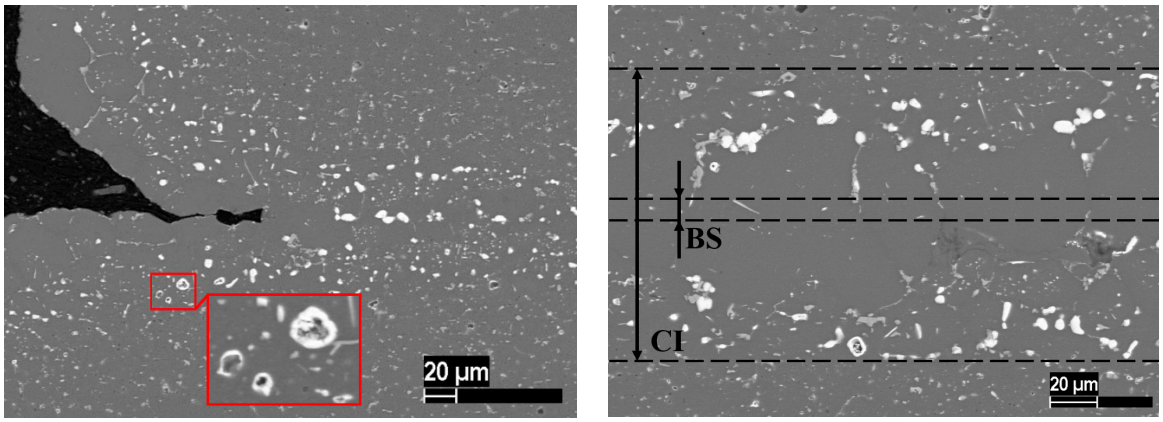

(**a**) (**b**)

Figure 7. Microstructure of the AA 6082/AA 6082 joint brazed according to the 540 °C/30 min mode, obtained by SEM at different magnifications: (**a**) 250× magnification; (**b**) 500× magnification.

The AA 6082/AA 6982 brazed joint microstructure was homogeneous. The AA 6082/AA 6082 brazed seam was characterized by a small thickness ~10 µm (Figure 7a). No visible boundary between the base material and the brazed seam (BS zone, Figure 7b) could be seen at high magnifications. The diffusion of the filler alloy elements to the base material occurred during brazing. The formation of various segregations was the result of the diffusion process in the chemical interaction zone that was 70–80 µm thick (CI zone, Figure 7b). EDX analysis was conducted to study the CI zone of the AA 6082/AA 6982 brazed joint (Figure 8, Table 4).

Table 4. Results of EDX analysis of the AA 6082/AA 6082 brazed joint.

Measurement Point	Chemical Composition (at.%)					Phase Interpretation
	Al	Si	Ge	Fe	Mn	
Spectra 1, 2	53.8	3.0	42.8	0.2	0.2	Al-Ge eutectic
Spectrum 3	73.8	10.9	0.4	13.8	1.1	Al_7Fe_2Si
Spectrum 4	98.6	0.8	0.6	0.0	0.0	(Al)

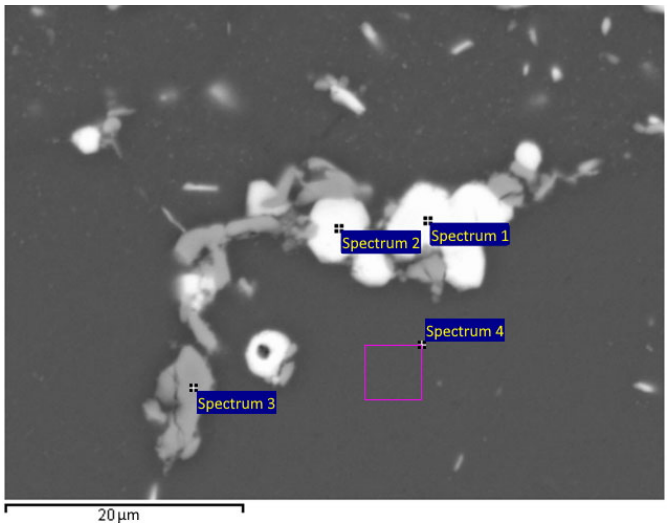

Figure 8. SEM image of the AA 6082/AA 6082 joint brazed according to the 540 °C/30 min mode with EDX measurement points.

The formation of the intermetallic compound corresponding to the stoichiometry Al_7Fe_2Si [2] in the CI zone was observed (Figure 8, spectrum 3). Germanium actively diffused into the aluminum alloy, where it precipitated with a composition close to the Al-Ge eutectic (Figure 8, spectrum 1, 2). The precipitates with a composition close to the Al-Ge eutectic was also obtained by Li [40]. However, the fine eutectic structure with different visible phases was not received using HAADF STEM [40]. The presence of such precipitates was observed in the CI zone at a significant distance from the brazed joint (Figure 7a). Some of the precipitates contained pores that shrunk during the crystallization of the low-melting Al-Ge eutectic (red area, Figure 7a).

Brazing, according to the 540 °C/30 min mode using Al-40.0Ge-3.4Si wt.% filler alloy foil, was carried out to study the formation of the stainless-steel (AISI 304/AISI 304) brazed joint (Figure 9). The thickness of the brazed seam was 50 ± 5 µm, and it was characterized by the absence of brazing defects. There were clearly visible boundaries between the steel and the brazed joint.

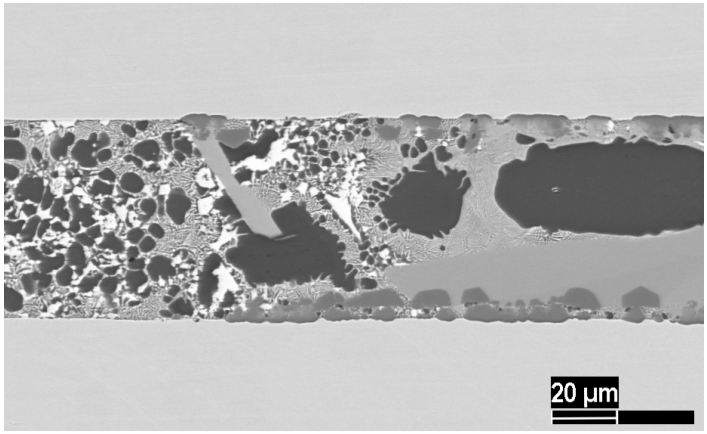

Figure 9. Microstructure of the AISI 304/AISI 304 joint brazed according to the 540 °C/30 min mode, obtained by SEM at 500× magnification.

Results of the EDX analysis of the AISI 304/AISI 304 brazed joint are shown in Figure 10 and Table 5. The steel surface was in contact with the Al_8Fe_2(Si, Cr) intermetallic compound with a thickness up to 10 µm (Figure 10, spectra 1–3), as well as a lamellar microstructure identical to the structure of the filler alloy ingot, consisting of eutectic

containing (Al, Ge) solid solution and pure Ge [22]. An inhomogeneous structure was formed in the central part of the brazed joint. It consisted of a eutectic structure containing an (Al)-based solid solution (Figure 10, spectra 6–7) and a (Ge, Si) solid solution (Figure 10, spectra 4–5). In addition, large Al-Ge eutectic segregations were formed in the center of the brazed seam (Figure 10, spectrum 8).

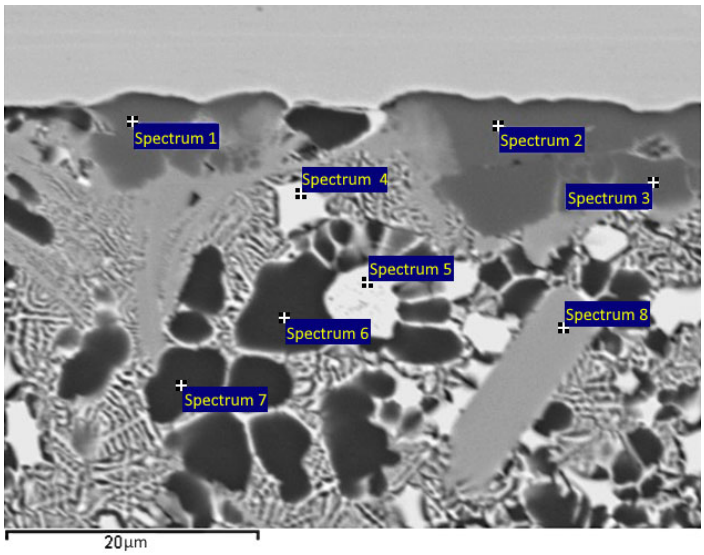

Figure 10. SEM image of the AISI 304/AISI 304 joint brazed according to the 540 °C/30 min mode with the EDX measurement points.

Table 5. Results of EDX analysis of the AISI 304/AISI 304 brazed joint.

Measurement Point	Chemical Composition (at.%)							Phase Interpretation
	Al	Si	Ge	Fe	Cr	Ni	Mn	
Spectra 1–3	70.9	8.6	2.1	13.6	4.2	0.3	0.3	Al_8Fe_2(Si, Cr)
Spectra 4, 5	3.7	5.2	89.8	0.8	0.2	0.2	0.1	(Ge, Si)
Spectra 6, 7	98.0	0.1	1.8	0.1	0.0	0.0	0.0	(Al)
Spectrum 8	67.0	0.6	28.9	2.0	0.3	1.1	0.1	Al-Ge eutectic

3.3. Dissimilar Material Brazing

Brazing, according to the 540 °C/30 min mode using Al-40.0Ge-3.4Si wt.% filler alloy foil, was carried out to study the aluminum alloy and stainless-steel (AISI 304/AA 6082) dissimilar joint formation features. The SEM microstructure of the AISI 304/AA6082 joint brazed at 540 °C/30 min at different magnifications is presented in Figure 11.

Results of the EDX analysis of the AISI 304/AA 6082 joint brazed at 540 °C/30 min mode are shown in Figure 12 and Table 6. The brazed joint was formed due to the formation of an Al_7Fe_2(Si, Cr) intermetallic compound layer that was 5–7 μm thick (Figure 12, spectra 9–11) during this brazing mode. The brazing process led to the formation of the Al-Ge eutectic structure in the near-surface layer of the aluminum alloy (Figure 12, spectra 1–3 and 7–8). The thickness of the near-surface layer containing Ge-rich precipitates was up to 200 μm (Figure 12, spectra 1–3). Moreover, the presence of precipitates with an Al-Ge eutectic composition with cavities and pores (red area, Figure 11b) was observed. Due to the high diffusion activity and the presence of iron in the composition of aluminum alloy AA 6082, the formation of Al_7Fe_2Si system intermetallic compound particles was observed in the area near the brazed joint, as well as deep in the aluminum alloy (Figure 12, spectra 4–6). The presence of the similar Al-Fe-Si intermetallic compounds in the aluminum alloy after induction brazing with steel was mentioned by Fedorov [2,37].

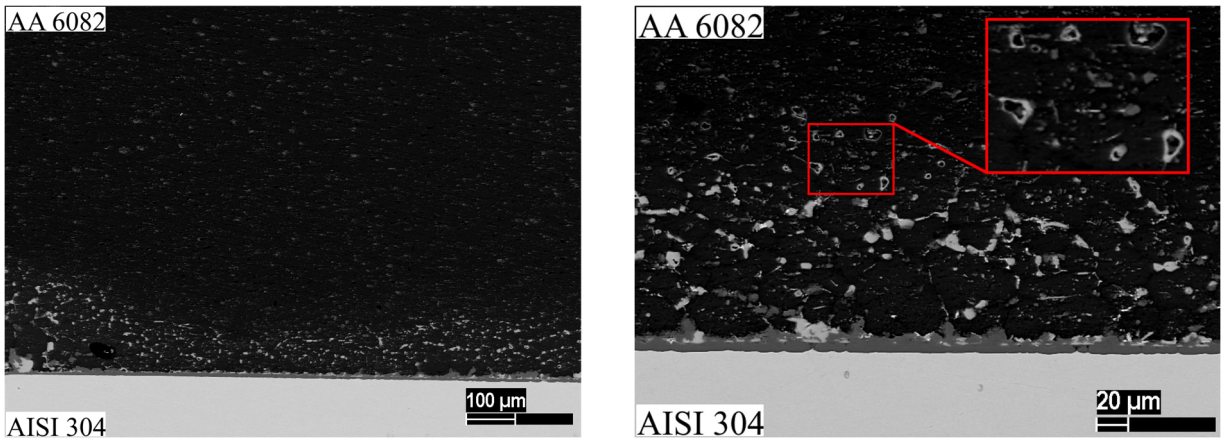

(**a**) (**b**)

Figure 11. Microstructure of the AISI 304/AA6082 joint brazed according to the 540 °C/30 min mode obtained by SEM at different magnifications: (**a**) 100× magnification; (**b**) 500× magnification.

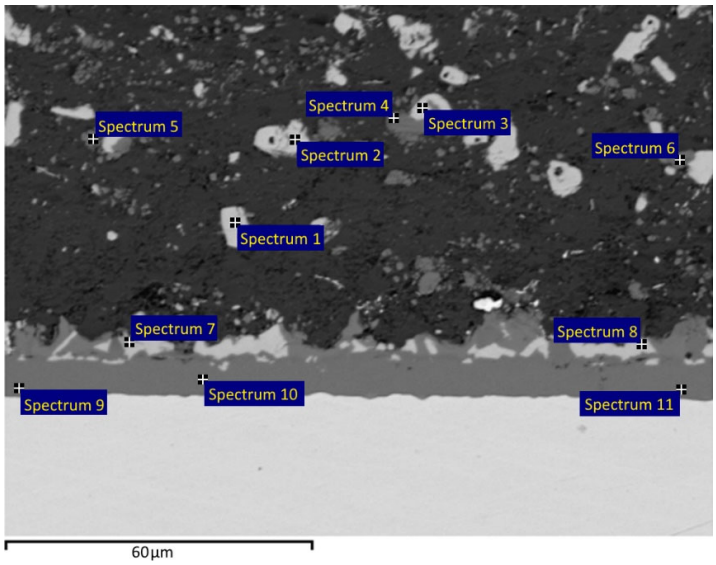

Figure 12. SEM image of the AISI 304/AA 6082 joint brazed according to the 540 °C/30 min mode with the EDX measurement points.

Table 6. Results of EDX analysis of the AISI 304/AA 6082 brazed joint.

Measurement Point	Chemical Composition (at.%)							Phase Interpretation
	Al	Si	Ge	Fe	Cr	Ni	Mn	
Spectra 1–3	59.5	3.9	33.0	0.0	3.5	0.0	0.2	Al-Ge eutectic
Spectra 4–6	66.2	10.4	0.3	16.6	1.2	0.0	3.3	Al_7Fe_2Si
Spectra 7, 8	58.4	2.9	32.5	0.0	6.2	0.0	0.0	Al-Ge eutectic
Spectra 9–11	61.4	8.0	0.6	21.0	8.4	0.3	0.3	Al_7Fe_2(Si, Cr)

High-strength aluminum alloys of the 6XXX series are age-hardenable alloys, and their mechanical characteristics are improved by heat treatment [41–43]. A common heat treatment for these alloys is the final heat treatment T6. This heat treatment consists of quenching in order to suppress the formation of intermediate phases, followed by aging, during which β′ and β″ particles are formed [42]. These particles are metastable modifications of the stable Mg_2Si phase, and obstruct the movement of dislocations [41,42].

Peng [21] carried out the final heat treatment of an AA 6063 aluminum alloy brazed joint after the brazing process. These compounds showed a strength of ~150 MPa. The formation of large brittle phases in the aluminum alloy during slow cooling negatively affects strength. It is possible to suppress this process by fast cooling after brazing exposure. Thus, the optimization of the brazing process will be carried out in future work. It is assumed that an additional final heat treatment would consist of quenching and subsequent artificial aging. However, this article focuses on the dissimilar brazed joint formation mechanism and brazing effects. Therefore, no additional heat treatment was carried out in this paper.

BSD images of the AISI 304/AA6082 joint brazed according to the 540 °C/30 min mode are shown in Figure 13.

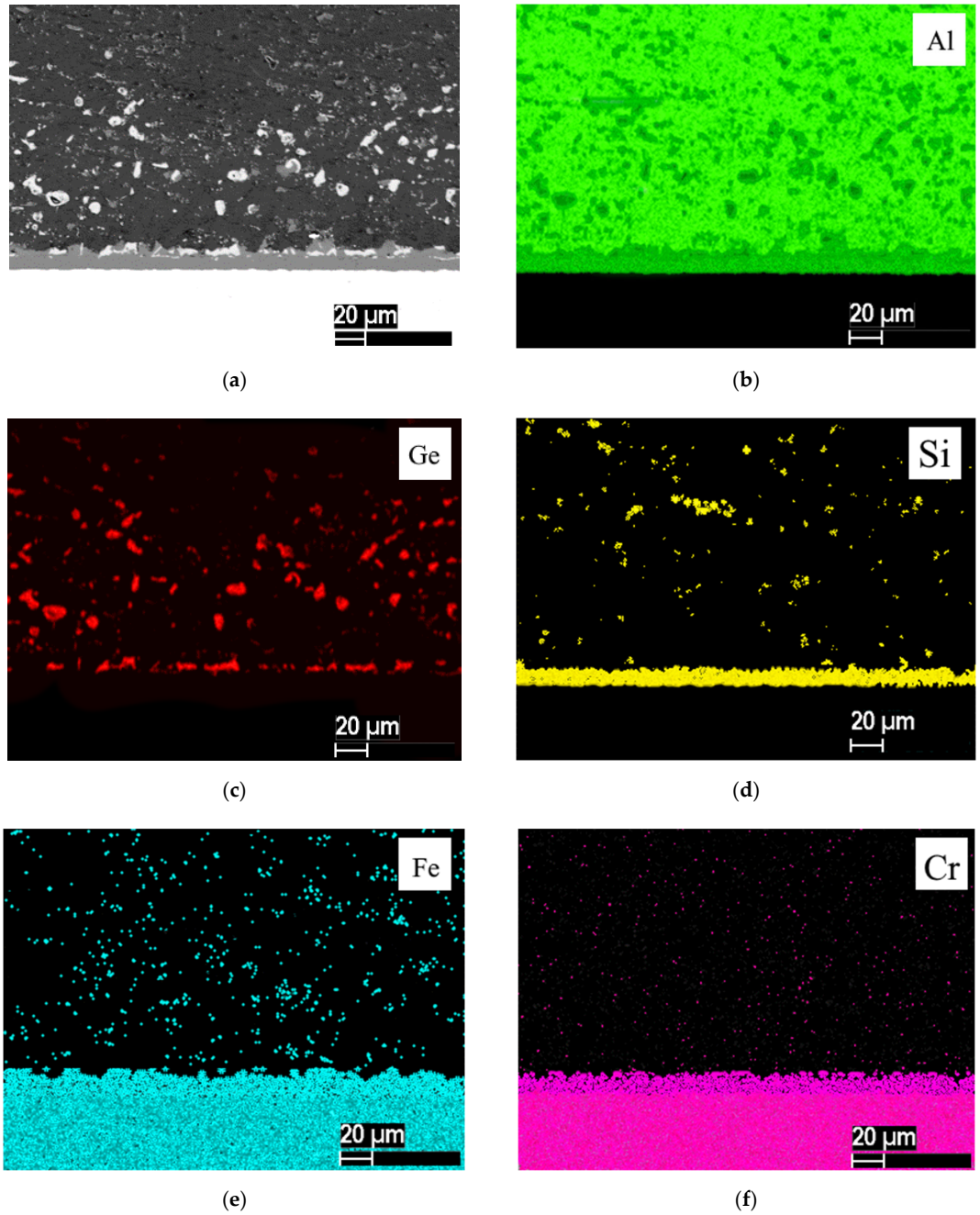

Figure 13. BSD image of the AISI 304/AA 6082 joint brazed according to the 540 °C/30 min mode at 1000× magnification: (**a**) initial image; (**b**) distribution of Al; (**c**) distribution of Ge; (**d**) distribution of Si; (**e**) distribution of Fe; (**f**) distribution of Cr.

Chemical distribution maps indicate that germanium does not participate in the formation of the brazed joint seam, and therefore, it was concluded that the presence of germanium in filler alloys affects only the critical temperatures of phase transformation (Figure 13c).

3.4. The Time–Temperature Effect on the Brazed Joints Microstructure

Microstructures of the AISI 304/AA6082 joints brazed according to the different modes obtained by SEM at ×1000 magnification are shown in Figure 14.

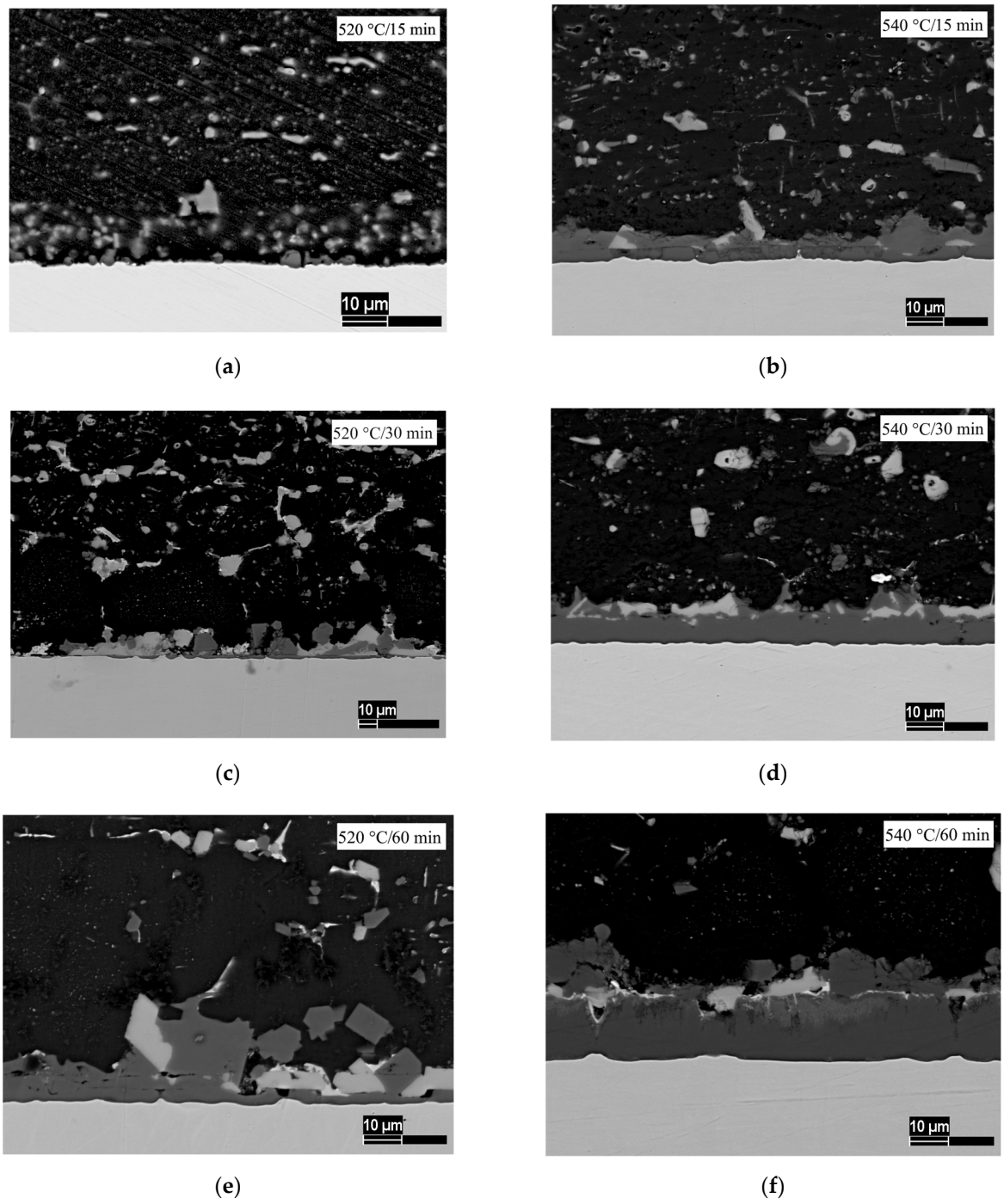

Figure 14. Microstructures of the AISI 304/AA6082 joints brazed according to the different modes obtained by SEM at 1000× magnification: (**a**) 520 °C/15 min; (**b**) 540 °C/15 min; (**c**) 520 °C/30 min; (**d**) 540 °C/30 min; (**e**) 520 °C/60 min; (**f**) 540 °C/60 min.

Brazing at 540 °C and 520 °C with exposure for 15, 30, and 60 min was carried out to study the relationship between the time–temperature brazing modes and the characteristics of the intermetallic compound reaction layer of AISI 304/AA 6082 brazed joints. Samples brazed according to the 520 °C/15 min mode showed the formation of the reaction layer with a thickness of 0.5–0.75 µm at the aluminum alloy and stainless-steel boundary, as well as larger particles of the Al_7Fe_2Si intermetallic compound at the border zone. The filler alloy was completely dissolved and its elements were redistributed during brazing (Figure 14a). The formation of a reaction layer and a further increase in its thickness to values of 1.5–2.0 µm and 3–7 µm were observed with an increase in the holding time to 30 and 60 min, respectively, at the same temperature (Figure 14c,e). Samples brazed according to the 540 °C/15 min mode showed the formation of the reaction layer with a thickness of 5–8 µm (Figure 14b). An increase in holding time to 30 and 60 min at this temperature led to growth in the reaction layer thickness to 7–10 µm and 15–18 µm, respectively (Figure 14d,f). The dependence of the reaction layer thickness on the holding time at different brazing temperatures is shown in Figure 15. An increase in the brazing temperature by 20 degrees led to a sharp growth in the reaction layer thickness to values close to critical numbers (10 µm). Nevertheless, brazed joints with a reaction layer up to 10 µm could obtain sufficient strength characteristics [2,5]. In this regard, joints obtained by 520 °C/15, 30 min and 540 °C/15, 30 min modes could obtain good mechanical characteristics.

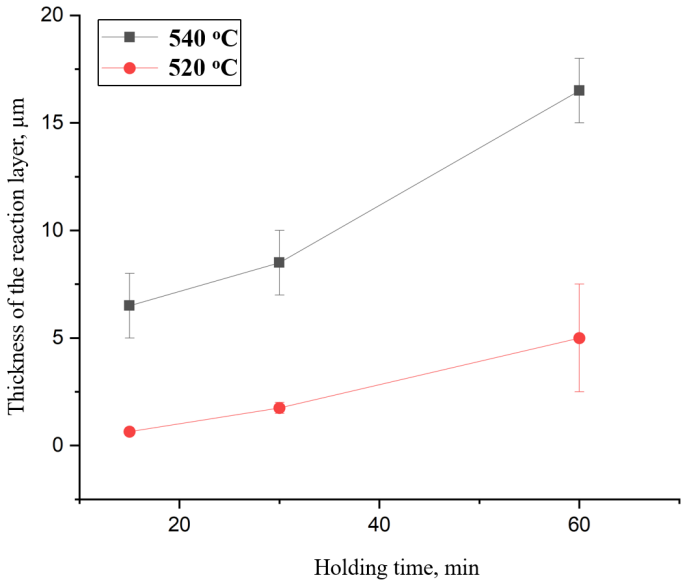

Figure 15. Dependence of the reaction layer width on the holding time during brazing at different temperatures.

3.5. AISI 304/AA 6082 Brazed Joint Formation Scheme

Figure 16 shows the proposed scheme for the AISI 304/AA 6082 brazed joint formation. A schematic diagram of element redistribution during brazing is presented in Figure 16a. The EDX analysis results (Figure 12, spectrum 7–8) showed that germanium-rich particles obtained a composition close to the Al-Ge eutectic (Al-28 Ge wt.% according to the state diagram). Melting of the Al-Ge-Si system filler alloys proceeded in two stages, as shown in previous work [22]. The first stage consisted of melting the Al-Ge eutectic at the temperature of 420 °C. The second stage consisted of melting the complex residue containing Al, Ge, and Si. Therefore, active Ge diffusion began at the melting temperature of the Al-Ge eutectic (420 °C) during the brazing of AISI 304 with AA 6082. Due to the penetration of germanium along the AA 6082 grain boundaries, these boundaries melted (yellow arrows, Figure 16b). The formation of a thin reaction layer of the Al-Fe-Si-Cr intermetallic compound was observed at the brazing temperature of 540 °C due to the diffusion of Al and Si from the filler alloy to the steel surface (red arrows, Figure 16b). During holding at the brazing

temperature (540 °C), the surface between the aluminum alloy and melt filler alloy moved toward the steel due to the redistribution of Al, Si, and Ge from the filler alloy, which led to the crystallization of the liquid phase (blue arrows, Figure 16b). Thus, in the 420–540 °C temperature range, the brazed seam—represented by the intermetallic compound reaction layer on the steel surface—whose thickness depends on the holding time during brazing and the aluminum matrix with liquid-phase inclusions, obtained a composition close to the Al-Ge eutectic (Figure 16c). It is important to note that the growth of the intermetallic compound reaction layer was located in the steel surface direction and was caused by the diffusion of aluminum atoms to steel (black arrows, Figure 16c). The increase in the reaction layer thickness was noted by Fedorov during the heat treatment of the aluminum alloy and steel joints below the brazing temperature [2]. The crystallization of the Al-Ge eutectic occurred after cooling below 420 °C (Figure 16d). Contraction during crystallization of the liquid could explain the pore formation in the Al-Ge particles (red area, Figure 16d). Complete isothermal solidification of the brazed seam could occur due to germanium migration into the AA 6082 alloy and the growth of the Al-Fe-Si-Cr reaction layer on the steel surface during the significant holding time of brazing.

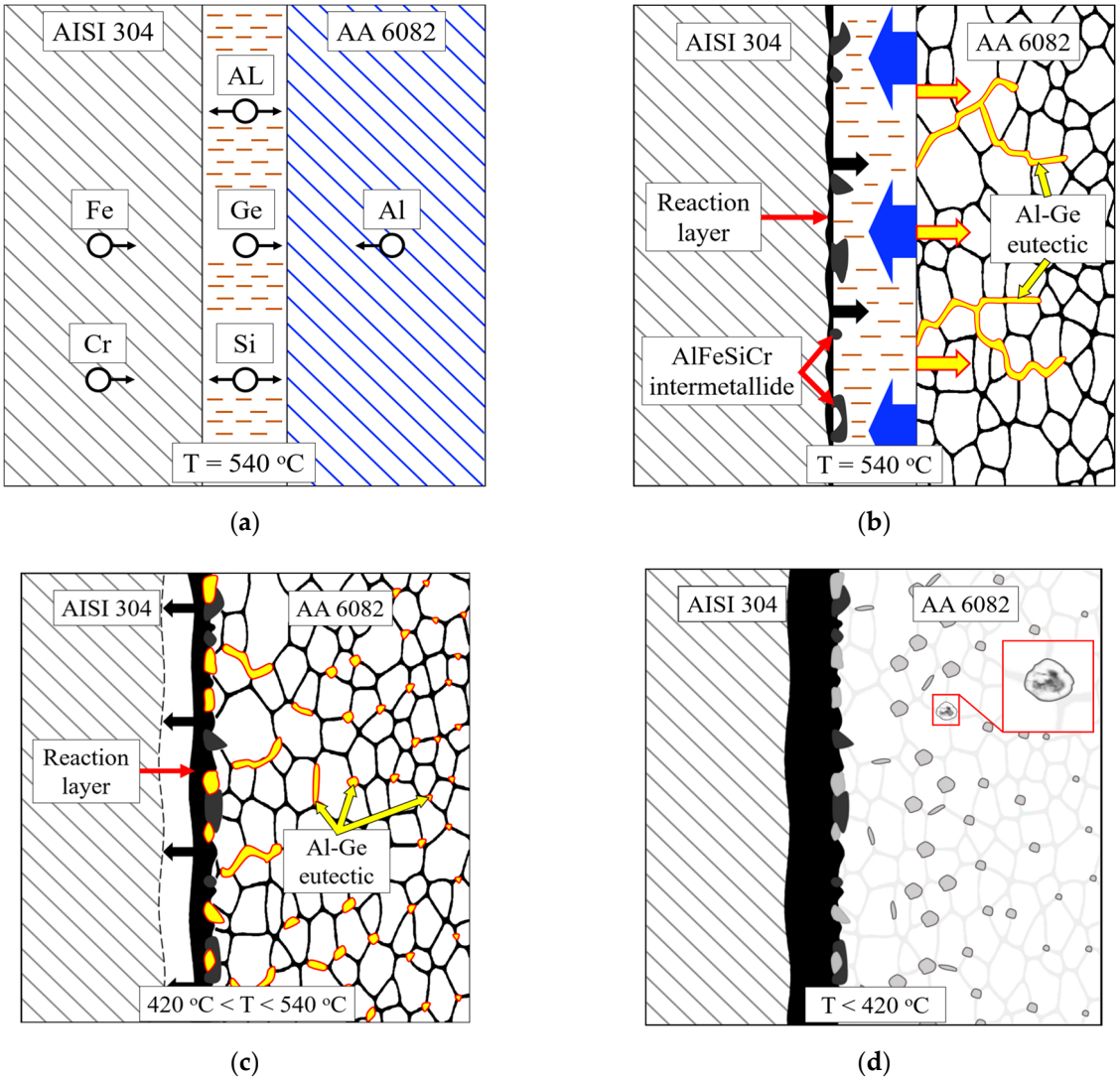

Figure 16. Scheme of the AISI 304/AA 6082 joint formation: (**a**) initial structure; (**b**) formation of the seam; (**c**) growth of the reaction layer; (**d**) final structure.

3.6. Mechanical Properties of the Brazed Joints

The fractogram with z-contrast and the destruction microstructure of the AA 6082/AA6082 joint brazed according to the 540 °C/30 min mode are presented in Figure 17. The strength of this joint was 42 ± 6 MPa. The fracture facets were elongated along the load application direction, indicating the viscous form of the brazed joint failure (Figure 17a). The presence of white-colored particles corresponding to the Al-Ge eutectic structure was observed on the rupture surface (Figure 8, spectra 1–2). The fracture microstructure indicated that the fracture passed through the chemical interaction zone (Figure 17b). The fracture surface also passed along the chemical interaction zone particle boundaries, pointing out their negative effect on the strength of the brazed joint (red arrows, Figure 17b).

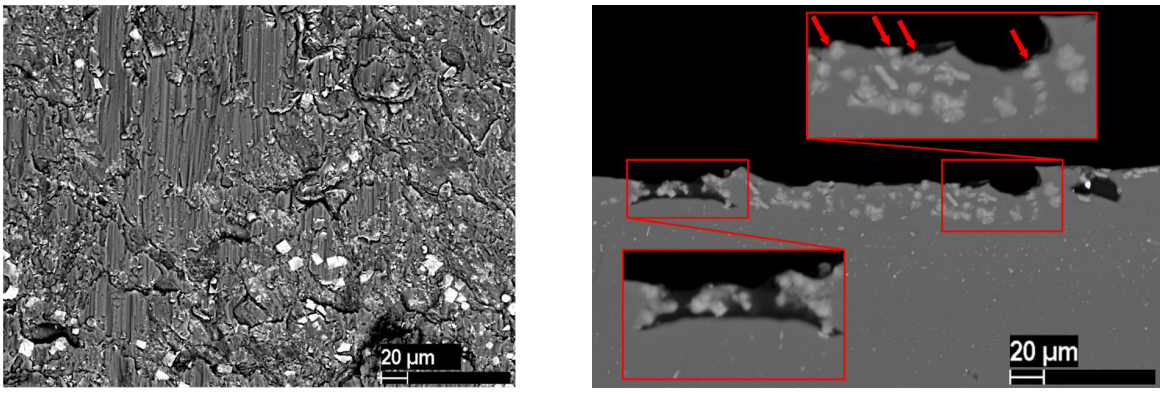

(**a**) (**b**)

Figure 17. SEM images of the AA 6082/AA 6082 joint brazed according to the 540 °C/30 min mode. Different fracture views at 1000× magnification: (**a**) surface fractogram with z-contrast; (**b**) cross-section.

The fractogram and destruction microstructure of the AISI 304/AISI 304 joint brazed according to the 540 °C/30 min mode are presented in Figure 18. The strength of this joint was 20 ± 4 MPa. The destruction surface consisted of many flat particles randomly located on the destruction surface (Figure 18a), indicating the brittle form of the joint destruction. Destruction was found along the reaction layer on both sides of the brazed joint. Crack formation was observed between various structural components: the (Ge, Si) solid solution with a high Ge content, the Al-Fe-Si-Cr reaction layer, and the (Al) solid solution (red arrows, Figure 18b). It should be noted that cracks were also located in steel close to the reaction layer (yellow arrows, Figure 18b).

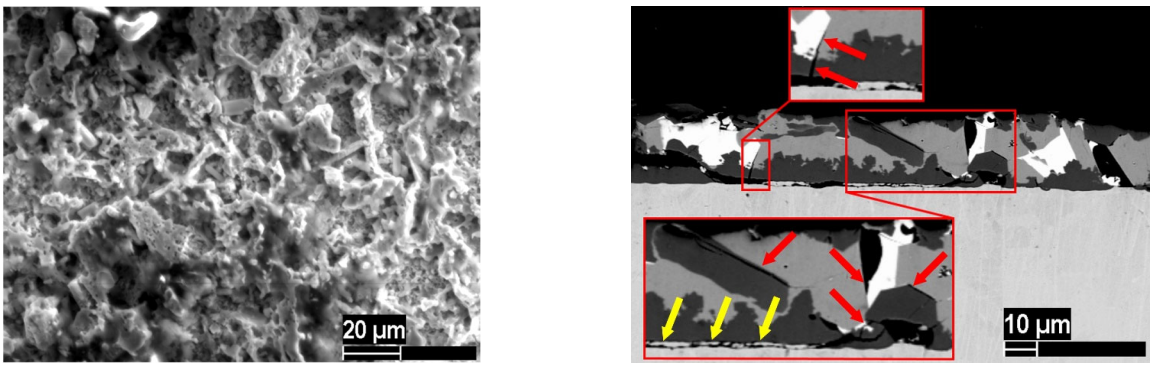

(**a**) (**b**)

Figure 18. SEM images of the AISI 304/AISI 304 joint brazed according to the 540 °C/30 min mode. Different fracture views at 1000× magnification: (**a**) surface fractogram; (**b**) cross-section.

The fractogram with z-contrast and the destruction microstructure of the AISI 304/AA6082 joint brazed according to the 540 °C/30 min mode are presented in Figure 19. The strength of this joint was 12 ± 3 MPa. The fracture passed through the reaction layer that was clearly visible on the fracture surface due to the z-contrast (Figure 19a). The fracture surface comprised the Al-Fe-Si-Cr intermetallic compound and stainless-steel surface flat sections. The fracture microstructure also showed the rupture surface located in the reaction layer (Figure 19b). Thus, the strength of the AISI 304/AA 6082 joint brazed according to the 540 °C/30 min mode was determined by the strength of the reaction layer, which depends on thickness.

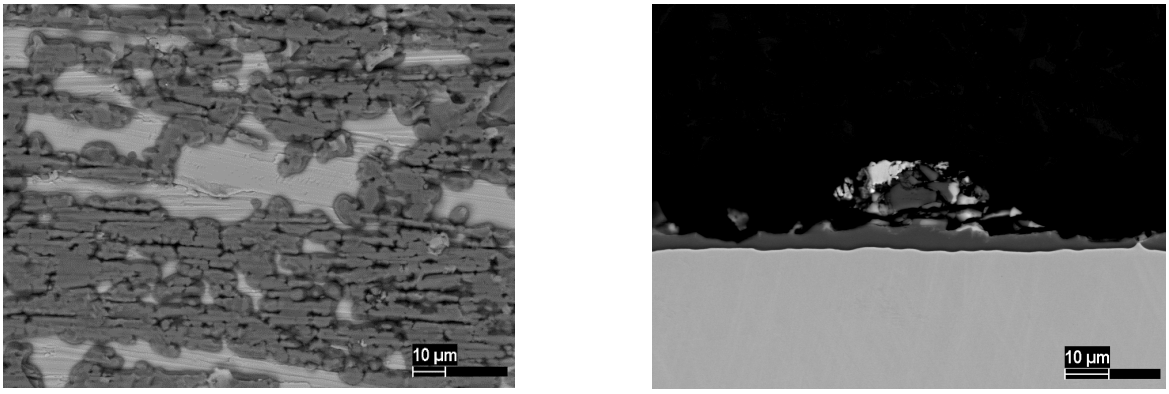

(**a**) (**b**)

Figure 19. SEM images of the AISI 304/AA 6082 joint brazed according to the 540 °C/30 min mode. Different fracture views at 1000× magnification: (**a**) surface fractogram with z-contrast; (**b**) cross-section.

4. Conclusions

The wetting experiment on the aluminum alloy AA6082 substrate with Al-40.0Ge-3.4 Si wt.% filler alloy demonstrated complete wetting with a 0° angle. The interaction of the filler alloy with the aluminum alloy led to the diffusion of germanium along the grain boundaries and the formation of low-melting Al-Ge eutectic, causing significant erosion of the base material. The formation of a drop with a wetting angle of 30 ± 5° was observed during the wetting of the stainless-steel AISI 304 substrate. The chemical interaction zone consisted of the Al_8Fe_2(Si, Cr) system reaction layer formed on the steel surface and the Al-Ge eutectic.

The microstructure of the AA 6082/AA6082 brazed joint was homogeneous. The formation of Al_7Fe_2Si intermetallic compound particles and Al-Ge eutectic composition particles was observed in the chemical interaction zone. This connection, obtained by brazing according to the 540 °C/30 min mode, had a strength of 42 ± 6 MPa. The destruction had a viscous form. The microstructure of the AISI 304/AISI 304 brazed joint was heterogeneous. The brazed joint formed due to the formation of the Al_8Fe_2(Si, Cr) intermetallic compound reaction layer on the steel surface. This connection obtained by brazing according to the 540 °C/30 min mode had a strength of 20 ± 4 MPa. The destruction was brittle, and the fracture surface passed through the reaction layer.

The proposed scheme for AISI 304/AA 6082 brazed joint formation was provided. This joint was formed due to the formation of a thin reaction layer on the steel surface at short holding times. Further growth of the reaction layer was realized mainly due to the diffusion of aluminum atoms to steel with the holding time increase. An increase in the brazing temperature with the same holding time led to a sharp increase in the reaction layer thickness. Germanium did not participate in the brazed seam formation. Its content in the Al-Ge-Si system filler alloys affected only the critical temperatures of phase transformation. The AISI 304/AA 6082 compound, obtained according to the 540 °C/30 min mode, had a strength of 12 ± 3 MPa. The destruction was brittle and passed through the reaction

layer. The strength of the AISI 304/AA 6082 joint, brazed according to the 540 °C/30 min mode, was determined by the strength of the reaction layer. Time–temperature brazing mode optimization in order to improve mechanical characteristics will be considered in future work. The formation of a diffusion barrier (protective coating) on the surface of the aluminum alloy has been proposed to eliminate erosion related to Ge diffusion. Such a method could reduce the negative effect of germanium diffusion into the aluminum alloy, and slow down the process of the growth of the reaction layer on the steel surface.

Author Contributions: Conceptualization, O.S. and A.I.; methodology, A.I., M.P. and A.S.; software, N.P. (Nikita Popov) and N.P. (Natalia Pukhareva); validation, A.I. and N.P. (Nikita Popov); formal analysis, A.I., A.A., N.P. (Nikita Popov) and N.P. (Natalia Pukhareva); investigation, A.I., A.A., N.P. (Nikita Popov) and N.P. (Natalia Pukhareva); resources, A.I., M.P. and A.S.; data curation, A.I., M.P. and N.P. (Nikita Popov); writing—original draft preparation, A.A. and N.P. (Nikita Popov); writing—review and editing, A.I., N.P. (Nikita Popov) and M.P.; visualization, A.A. and N.P. (Natalia Pukhareva); supervision, O.S., A.I. and A.S.; project administration, O.S., A.I. and A.S.; funding acquisition, A.S., O.S., A.I. and M.P. All authors have read and agreed to the published version of the manuscript.

Funding: The reported study was funded by RFBR and DFG, project number 21-52-12026.

Data Availability Statement: The data are contained within the article.

Conflicts of Interest: The authors declare no conflict of interest.

References

1. Taban, E.; Gould, J.E.; Lippold, J.C. Dissimilar friction welding of 6061-T6 aluminum and AISI 1018 steel: Properties and microstructural characterization. *Mater. Des.* **2010**, *31*, 2305–2311. [CrossRef]
2. Fedorov, V.; Uhlig, T.; Wagner, G. Influence of the thickness of the reaction zone in aluminum/stainless steel brazed joints on themechanical properties. *Metals* **2021**, *11*, 217. [CrossRef]
3. Miller, W.S.; Zhuang, L.; Bottema, J.; Wittebrood, A.J.; De Smet, P.; Haszler, A.; Vieregge, A. Recent development in aluminium alloys for the automotive industry. *Mater. Sci. Eng. A* **2000**, *280*, 37–49. [CrossRef]
4. Kobayashi, S.; Yakou, T. Control of intermetallic compound layers at interface between steel and aluminum by diffusion-treatment. *Mater. Sci. Eng. A* **2002**, *338*, 44–53. [CrossRef]
5. Schubert, E.; Klassen, M.; Zerner, I.; Walz, C.; Sepold, G. Light-weight structures produced by laser beam joining for future applications in automobile and aerospace industry. *J. Mater. Process. Technol.* **2001**, *115*, 2–8. [CrossRef]
6. Fridlyander, I.N.; Sister, V.G.; Grushko, O.E.; Berstenev, V.V.; Sheveleva, L.M.; Ivanova, L.A. Aluminum alloys: Promising materials in the automotive industry. *Met. Sci. Heat Treat.* **2002**, *44*, 365–370. [CrossRef]
7. Dong, H.; Yang, L.; Dong, C.; Kou, S. Improving arc joining of Al to steel and Al to stainless steel. *Mater. Sci. Eng. A* **2012**, *534*, 424–435. [CrossRef]
8. Liu, J.; Jiang, S.; Shi, Y.; Kuang, Y.; Huang, G.; Zhang, H. Laser fusion-brazing of aluminum alloy to galvanized steel with pure Al filler powder. *Opt. Laser Technol.* **2015**, *66*, 1–8. [CrossRef]
9. Rathod, M.J.; Kutsuna, M. Joining of Aluminum Alloy 5052 and Low-Carbon Steel by Laser Roll Welding. *Weld. J.* **2004**, *83*, 16–26.
10. Tanaka, T.; Morishige, T.; Hirata, T. Comprehensive analysis of joint strength for dissimilar friction stir welds of mild steel to aluminum alloys. *Scr. Mater.* **2009**, *61*, 756–759. [CrossRef]
11. Lee, W.B.; Schmuecker, M.; Mercardo, U.A.; Biallas, G.; Jung, S.B. Interfacial reaction in steel-aluminum joints made by friction stir welding. *Scr. Mater.* **2006**, *55*, 355–358. [CrossRef]
12. Watanabe, T.; Takayama, H.; Yanagisawa, A. Joining of aluminum alloy to steel by friction stir welding. *J. Mater. Process. Technol.* **2006**, *178*, 342–349. [CrossRef]
13. Thoma, M.; Wagner, G.; Strab, B.; Wolter, B.; Benfer, S.; Furbeth, W. Hybrid Al/steel-joints manufactured by ultrasound enhanced friction stir welding (USE-FSW): Process comparison, nondestructive testing and microscopic analysis. *J. Phys. Conf. Ser.* **2016**, *755*, 011001. [CrossRef]
14. Song, J.L.; Lin, S.B.; Yang, C.L.; Fan, C.L. Effects of Si additions on intermetallic compound layer of aluminum-steel TIG welding-brazing joint. *J. Alloys Compd.* **2009**, *488*, 217–222. [CrossRef]
15. Mathieu, A.; Shabadi, R.; Deschamps, A.; Suery, M.; Matteï, S.; Grevey, D.; Cicala, E. Dissimilar material joining using laser (aluminum to steel using zinc-based filler wire). *Opt. Laser Technol.* **2007**, *39*, 652–661. [CrossRef]
16. Lü, J.; Yang, W.; Wu, S.; Zhao, X.; Xiao, R. Microstructure and mechanical properties of galvanized steel/AA6061 joints by laser fusion brazing welding. *Acta Metall. Sin.* **2014**, *27*, 670–676. [CrossRef]
17. Fedorov, V.; Uhlig, T.; Wagner, G. Investigation of fatigue damage in aluminum/stainless steel brazed joints. *Weld. World* **2018**, *62*, 609–616. [CrossRef]

18. Dai, W.; Xue, S.; Lou, J.; Wang, S. Microstructure and properties of 6061 aluminum alloy brazing joint with alsizn filler metal. *Mater. Trans.* **2012**, *53*, 1638–1643. [CrossRef]
19. Humpston, G. New filler metals and and process for fluxless brazing of aluminum engineering alloys. *Mater. Sci. Technol.* **1995**, *11*, 1161–1168. [CrossRef]
20. Bae, S.C.; Whang, J.I.; Reif, W. Study on the high frequency induction brazing of aluminum with AlSi filler metals. *Metall* **2002**, *56*, 564–569.
21. Peng, C.; Zhu, D.; Li, K.; Du, X.; Zhao, F.; Wan, M.; Tan, Y. Research on a low melting point al-si-cu (Ni) filler metal for 6063 aluminum alloy brazing. *Appl. Sci.* **2021**, *11*, 4296. [CrossRef]
22. Ivannikov, A.; Fedorov, V.; Abramov, A.; Penyaz, M.; Bachurina, D.; Uhlig, T.; Suchkov, A.; Wagner, G.; Morokhov, P.; Sevryukov, O. Development of Rapidly-Quenched Al-Ge-Si Filler Alloys for the Joining of Stainless Steel AISI 304 and Aluminum Alloy. *Metals* **2021**, *11*, 1926. [CrossRef]
23. Hornbogen, E.; Mukhopadhyay, A.K.; Starke, E.A. Precipitation hardening of Al-(Si, Ge) alloys. *Scr. Metall. Mater.* **1992**, *27*, 733–738. [CrossRef]
24. Kayamoto, T.; Kim, J.-H.; Saito, S.; Onzawa, T. Brazing of Al-Mg alloy and Al-Mg-Si alloy with Al-Ge based filler metals. *Q. J. Jpn. Weld. Soc.* **1994**, *12*, 495–501. [CrossRef]
25. Niu, Z.; Huang, J.; Yang, H.; Chen, S.; Zhao, X. Preparation and Properties of a Novel Al-Si-Ge-Zn Filler Metal for Brazing Aluminum. *J. Mater. Eng. Perform.* **2015**, *24*, 2327–2334. [CrossRef]
26. Hayes, F.H.; Longbottom, R.D.; Ahmad, E.; Chen, G. On the Al-Si, Al-Ge, and Al-Ge-Si systems and their application to brazing in high power semiconductor devices. *J. Phase Equilibria* **1993**, *14*, 425–431. [CrossRef]
27. Niu, Z.; Huang, J.; Chen, S.; Zhao, X. Effects of germanium additions on microstructures and properties of Al–Si filler metals for brazing aluminum. *Trans. Nonferrous Met. Soc. China* **2016**, *26*, 775–782. [CrossRef]
28. Xu, R.; Zhao, H.; Li, J.; Liu, R.; Wang, W.K. Microstructures of the eutectic and hypereutectic Al-Ge alloys solidified under different pressures. *Mater. Lett.* **2006**, *60*, 783–785. [CrossRef]
29. Stepanov, V.V. Development of Al-Si-Ge System Solders for Increasing the Strength of Brazed Structures Made of Aluminum Alloys. Master's Thesis, Moscow State Aviation Technological University, Moscow, Russia, 2006.
30. Zhang, Y.; Gao, T.; Liu, X. Influence of Ge content on the microstructure, phase formation and microhardness of hypereutectic Al-Si alloys. *J. Alloys Compd.* **2014**, *585*, 442–447. [CrossRef]
31. Kalin, B.; Fedotov, V.; Sevruykov, O.; Mamedova, T.; Rybkin, B.; Ivanov, A.; Timoshin, S. Development and application of rapidly-quenched filler alloys for precision brazing of dissimilar materials of nuclear technology. *Issues Sci. Technol* **2005**, *5*, 150–155.
32. Kalin, B.; Fedotov, V.; Sevruykov, O. Development and rapidly-quenched alloys application for brazing and cladding of nuclear technology structural elements. In Proceedings of the 4th International Scientific and Technical Conference Ensuring the Safety of Nuclear Power Plants with the WWER, «GIDROPRESS», Podolsk, Russia, 23–26 May 2005.
33. Martinsen, K.; Hu, S.J.; Carlson, B.E. Joining of dissimilar materials. *CIRP Ann. Manuf. Technol.* **2015**, *64*, 679–699. [CrossRef]
34. Agudo, L.; Eyidi, D.; Schmaranzer, C.H.; Arenholz, E.; Jank, N.; Bruckner, J.; Pyzalla, A.R. Intermetallic Fe x Al y -phases in a steel/Al-alloy fusion weld. *J. Mater. Sci.* **2007**, *42*, 4205–4214. [CrossRef]
35. Fedorov, V.; Weis, S.; Wagner, G. Mechanical and microstructural behavior of brazed aluminum / stainless steel mixed joints. *IOP Conf. Ser. Mater. Sci. Eng.* **2016**, *118*, 3–8. [CrossRef]
36. Roulin, M.; Luster, J.W.; Karadeniz, G.; Mortensen, A. Strength and structure of furnace-brazed joints between aluminum and stainless steel. *Weld. J.* **1999**, *78*, 151–155.
37. Fedorov, V.; Uhlig, T.; Wagner, G. Interfacial microstructure and mechanical properties of brazed aluminum/stainless steel joints. *J. Phys. Conf. Ser.* **2017**, *755*, 3–9. [CrossRef]
38. Fedorov, V.; Uhlig, T.; Wagner, G. Joining of aluminum and stainless steel using AlSi10 brazing filler: Microstructure and mechanical properties. *AIP Conf. Proc.* **2017**, *1858*, 030005. [CrossRef]
39. Akdeniz, M.V.; Mekhrabov, A.O. The effect of substitutional impurities on the evolution of Fe-Al diffusion layer. *Acta Mater.* **1998**, *46*, 1185–1192. [CrossRef]
40. Li, J.; Wanderka, N.; Balogh, Z.; Stender, P.; Kropf, H.; Albu, M.; Tsunekawa, Y.; Hofer, F.; Schmitz, G.; Schumacher, P. Effects of Trace Elements (Y and Ca) on the Eutectic Ge in Al-Ge Based Alloys. *Acta Mater.* **2016**, *111*, 85–95. [CrossRef]
41. Chen, C.H.; Sun, Y.K.; Lai, Y.C.; Chang, S.Y.; Chuang, T.H. Effect of post-weld heat treatment on the solid-state diffusion bonding of 6061 aluminum alloy. *Appl. Sci.* **2021**, *11*, 9660. [CrossRef]
42. Zupanič, F.; Steinacher, M.; Žist, S.; Bončina, T. Microstructure and properties of a novel Al-Mg-Si alloy aa 6086. *Metals* **2021**, *11*, 368. [CrossRef]
43. Kim, Y.M.; Choi, S.W.; Kim, Y.C.; Kang, C.S.; Hong, S.K. Influence of the precipitation of secondary phase on the thermal diffusivity change of Al-Mg2Si alloys. *Appl. Sci.* **2018**, *8*, 2039. [CrossRef]